Magnetic properties of the $(Cr_{100-x}Al_x)_{99}V_1$ alloy system

B Muchono[1,2], C J Sheppard[1], A R E Prinsloo[1] and H L Alberts[1]

[1] Physics Department, University of Johannesburg, P.O. Box 524, Auckland Park, Johannesburg 2006, South Africa
[2] Applied Physics Department, NUST, Box AC939, Ascot, Bulawayo, Zimbabwe

E-mail address: alettap@uj.ac.za

Abstract. Electrical resistivity (ρ), Seebeck coefficient (S) and magnetic susceptibility (χ) measurements as a function of temperature on the $(Cr_{100-x}Al_x)_{99}V_1$ alloy system, with $0 < x < 7$ are reported. Néel temperatures (T_N) obtained from all these measurements decrease with Al concentration, disappearing near $x \approx 1.5$, again reappearing for $x > 4.0$. $\rho(T)$ and $S(T)$ for samples with $x \geq 6.1$ show weak anomalies making the determination of T_N difficult. However, these anomalies are sharply defined in $\chi(T)$, proving that it is an important tool in probing antiferromagnetic in this system. The present results show that the addition of just 1 at.% V to the $Cr_{100-x}Al_x$ alloy system suppresses antiferromagnetism in the concentration range $1.5 \leq x \leq 4.0$. This behaviour is similar to that observed for the $(Cr_{100-x}Al_x)_{95}Mo_5$ alloy system.

1. Introduction

Cr and its dilute alloys are itinerant electron spin density wave antiferromagnetic materials [1]. The influence of Al in the Cr matrix is rather unique amongst Cr alloys in that increasing the Al content does not continuously decrease the Néel transition temperature T_N [1] as expected from the two-band theory [2]. However, T_N decreases sharply, reaches a minimum value of approximately 100 K at a critical concentration $x_c \approx 2$ at.% Al, where after it increases sharply on further addition of the Al content [1, 3]. The critical concentration lies at a deep minimum on the $Cr_{100-x}Al_x$ magnetic phase diagram. The critical concentration separates the incommensurate spin-density-wave (ISDW) phase for which $x \leq x_c$, the commensurate spin-density-wave (CSDW) phase for which $x \geq x_c$ and the paramagnetic (P) phase for which $T > T_N$ [1, 3, 4]. The interesting magnetic properties of this system were previously explored by the addition of 5 at.% Mo to form a $(Cr_{100-x}Al_x)_{95}Mo_5$ alloy system [5]. Antiferromagnetism (AFM) in this system was suppressed to below 4 K in the range $2 \leq x \leq 5$ [5]. Alloying with Mo suppresses AFM in Cr and its alloys through electron hole pair breaking effects due to electron scattering and through a delocalization of the 3-d bands of Cr by the 4-d bands of Mo [1]. For comparison, the present study investigates the magnetic properties of the $Cr_{100-x}Al_x$ system further through the addition of V. This reduces the AFM in Cr alloys through a mechanism different to that associated with Mo by reducing the electron-to-atom (e/a) ratio [1].

2. Experimental

Polycrystalline $(Cr_{100-x}Al_x)_{99}V_1$ alloys in the range $0 \leq x \leq 7$ were prepared by repeated arc melting in a purified argon atmosphere. The starting materials were Cr, Al and V of nominal purity 99.999%, 99.999% and 99.98%, respectively. The alloys were separately sealed into quartz ampoules filled with ultra-high purity argon and annealed at 1300 K for 72 hours after which they were quenched into iced water. Elemental composition analysis done using scanning electron microscopy and electron

microprobe showed that the alloys were of good homogeneity. Spark erosion techniques were used to cut, shape and polish the samples into desired dimensions for each experimental set-up. The Quantum Design Physical Property Measurement System (PPMS) was used to measure the electrical resistivity (ρ) and Seebeck coefficient (S) during cooling and heating runs, respectively, in the temperature range 2 K $\leq T \leq$ 390 K. The Quantum Design Magnetic Property Measurement System (MPMS) was used to measure the susceptibility (χ) in the temperature range 2 K $\leq T \leq$ 390 K. The samples were zero field cooled to 2 K and measurements were taken on warming in a magnetic field of 100 Oe.

3. Results and discussion

Figure 1 shows representative examples of the temperature dependence of the electrical resistivity, $\rho(T)$, for the $(Cr_{100-x}Al_x)_{99}V_1$ alloy system. Well defined resistivity anomalies, in the form of a 'hump', are observed in figure 1(a) and (b) in the vicinity of T_N at the P-ISDW phase transition for alloys with $x < 1.5$. These resistivity anomalies are ascribed to a reduction of charge carrier density during AFM ordering when the nested parts of the Fermi surface (FS) annihilate on cooling through T_N. The annihilation of the FS induces SDW energy gaps at the Fermi energy, causing an increase in the electrical resistivity just below T_N [1]. T_N shown in figures 1(a) and (b) was taken at the temperature of the sharp minimum in the $(d\rho/dT)$ vs. T curve as is usually done for Cr alloys [1]. No anomalous $\rho(T)$-behaviour was observed for alloys in the concentration range $1.5 \leq x \leq 4.7$ as shown by the typical example in figure 1(c). For these alloys, $\rho(T)$ is closely linear down to about 100 K, typical of what is expected for a paramagnetic Cr alloy [1]. The absence of $\rho(T)$-anomalies like that in figures 1(a) and (b) indicates paramagnetisn in this concentration range down to the lowest temperature of the

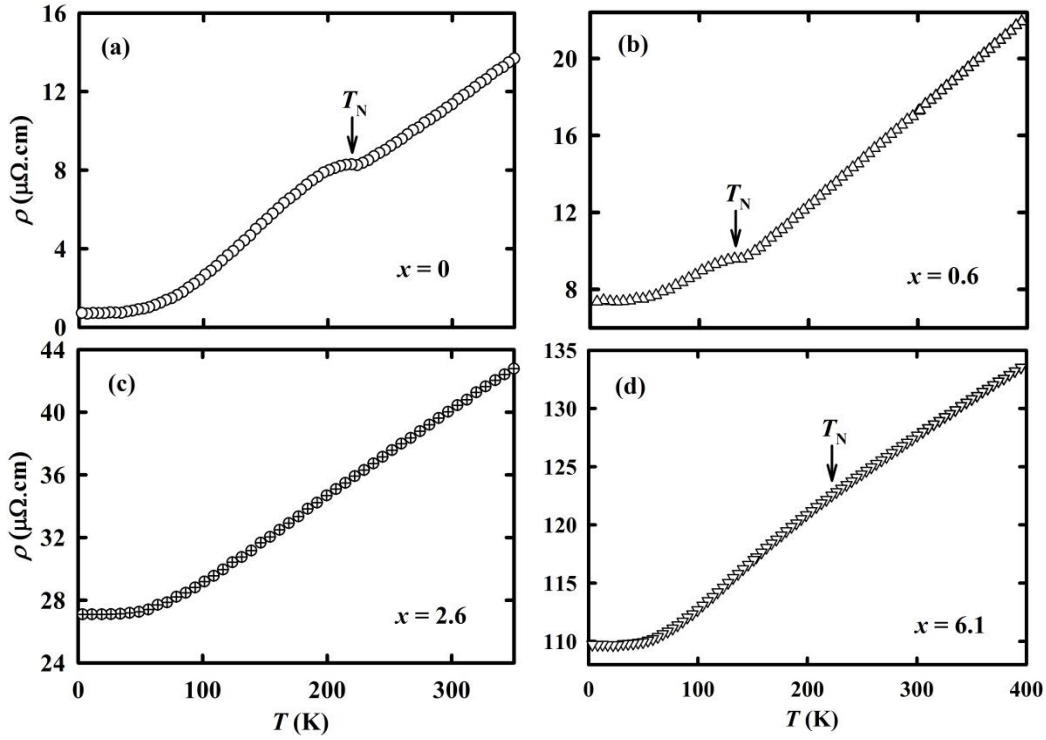

Figure 1: Representative examples of the temperature dependence of electrical resistivity, $\rho(T)$, of the $(Cr_{100-x}Al_x)_{99}V_1$ alloy system with (a) x = 0, (b) x = 0.6, (c) x = 2.6 and (d) x = 6.1. The arrows in panels (a) and (b) indicate the positions of T_N obtained from the minimum of the $(d\rho/dT)$ vs. T curves. T_N shown in panel (d) is obtained from Seebeck coefficient and magnetic susceptibility measurements of figures 2 and 3, respectively. The experimental error in ρ is approximately 5% originating from measurement of the sample dimensions. Note the different temperature scales.

measurements. For alloys with $x > 4.7$ $\rho(T)$ behave distinctly different from that observed for the previous two concentration ranges. A typical example is shown in figure 1(d) for $x = 6.1$ which, together with the $x = 7.0$ alloy, are expected to be CSDW AFM alloys. These two alloys show $\rho(T)$-behaviour that is characterized by a broad but weak anomaly in the form of a break in $d\rho/dT$ at a temperature marked "T_N" in the example of figure 1(d). This value of T_N corresponds very well with that obtained from Seebeck coefficient and magnetic susceptibility measurements of figures 2(d) and 3(b), respectively. A similar correspondence is obtained for T_N of the $x = 7.0$ alloy. It is unknown why T_N obtained from figures 2(d) and 3(b) correspond well with the break in $d\rho/dT$ for these two alloys, particularly since one would expect similar T_N-anomalies on $\rho(T)$ curves for both the ISDW and CSDW alloys. The downturn in $\rho(T)$ just below T_N for the CSDW alloys, instead of the expected upturn as for the ISDW alloys (figures 1(a) and (b)), is unexpected. Enhanced $\rho(T)$-anomalies, similar in form to that for the ISDW alloys, are rather expected for the P-CSDW T_N-anomaly, since the CSDW state is expected be more stable than the ISDW state [1]. Weak CSDW magnetic anomalies in $\rho(T)$ at T_N were previously also reported in the $Cr_{100-x}Al_x$ [6] and $(Cr_{100-x}Al_x)_{95}Mo_5$ [5, 7] alloy systems.

In some cases where the $\rho(T)$ magnetic anomalies are weak, Seebeck coefficient (S) measurements as a function of temperature provide a more sensitive method for locating T_N. Changes in the relaxation time τ of the itinerant charge carriers at the FS during AFM ordering is the dominant factor driving the enhanced anomaly observed in the $S(T)$ measurements [8].

The contribution to the Seebeck coefficient by electron diffusion is given by [1, 8]:

$$S = \frac{\pi^2 {k_B}^2 T}{3e}\left(\frac{\partial ln\Sigma}{\partial E} + \frac{\partial \bar{l}}{\partial E}\right)_{E_F}, \quad (1)$$

where Σ is the remaining FS area after annihilation due to electron-hole condensation and $\bar{l} = v\tau$ is the weighted average mean free path over Σ, v is the velocity of charge carriers at the remaining FS (Σ), and τ is the relaxation time. The two terms in equation (1) incorporating Σ and $\bar{l}$, are very sensitively affected on SDW formation in Cr and its alloys [8]. Σ is in many cases sensitive to the energy E, but for T just below T_N, where a 'hump' is observed in $\rho(T)$, the second term in equation (1) can dominate when the electron scattering may be largely determined by $\bar{l}$. At low temperatures a plot of S/T versus T^2 should then vary linearly [1, 8]:

$$S = aT + bT^3, \quad (2)$$

since both phonon and magnon drag in these itinerant electron AFM materials contribute T^3-terms to S at low temperatures [1, 8].

Previously investigated Cr alloys [1] all show $S(T)$ behaviour in the form of a relatively large 'dome' at $T < T_N$, compared to the small hump observed in $\rho(T)$. Trego *et al.* [8] discussed this behaviour in terms of a model in which the dominant effect is the decrease in the scattering rate of electrons by phonons when the AFM phase is entered on decreasing temperature. As indicated by equation. (1), S is determined by the energy dependence of both Σ and $\bar{l}$. The second term of equation (1) dominates [8] giving a net positive contribution to S at temperatures below T_N.

Figure 2 shows the temperature dependence of the Seebeck coefficient $S(T)$ for the $(Cr_{100-x}Al_x)_{99}V_1$ alloy system. Large anomalies in the form of a 'dome' are observed around the same region where the $\rho(T)$ curves showed a 'hump' for the alloys with $x < 1.5$ as indicated in figures 2(a) and (b). This 'dome' is as a result of a transition from P-ISDW phase as the alloys are cooled through T_N. The anomalies are small for alloys in the concentration range $1.5 \leq x \leq 4.7$ as shown in figure 2(b) and (c) (note the different scale on the S-axes of panels (b), (c) and (d) compared to that in panel (a)). These alloys show paramagnetic behaviour in the $\rho(T)$ measurements. The slight residue of a 'dome' observed in the $S(T)$ curves of the paramagnetic samples are at present not well understood, but was also observed in other Cr alloys [1, 8]. A noticeable and relatively sharp upturn is however present in $S(T)$ at temperatures larger than 150 K for x =1.5 in figure 2(b), compared to the behaviour observed for x = 2.6, 4.0 and 4.7. The electrical resistivity and magnetic susceptibility measurements of figures 2(c) and 3(a), respectively, nevertheless indicate paramagnetic behavior down to 2 K in the x = 1.5

alloy. Prominent anomalies reappear for alloys with $x > 4.7$ shown in figure 2(d). The magnetic anomalies observed in the $S(T)$ measurements are explained by Trego *et al.* [8] to result from the additional energy gaps that are formed during the annihilation of the nested parts of the FS. The energy gaps reduce the density of final states to which an electron can be scattered to, thereby increasing the mean free path as well as τ. The increase in the mean free path dominates the decrease in the FS area resulting in a positive magnetic contribution to $S(T)$ on cooling through T_N [8], explaining the 'domes' observed in figures 2(a) and (d). The magnetic anomalies observed in the $S(T)$ measurements of this alloy series are, as expected, better enhanced than those observed in the $\rho(T)$ measurements. The arrows in figure 2 indicate the positions of T_N values obtained from (dS/dT) vs. T curves. These values of T_N compare very well with those obtained from $\rho(T)$ measurements on assuming that T_N for $x = 6.1$ and 7.0 is taken at the temperature of the break in $d\rho/dT$, as in figure 1(d). This indicates that $\rho(T)$ and $S(T)$ measurements complement each other.

The study of magnetic properties of the $(Cr_{100-x}Al_x)_{99}V_1$ alloy system was extended to $\chi(T)$ measurements which give an indication of the density of states at the FS. Figure 3 shows the $\chi(T)$ curves for alloys with (a) $x \leq 2.6$ and (b) $x \geq 4.0$. The broken lines in figure 3 represent a back extrapolation from the paramagnetic phase at $T > T_N$. The T_N values indicated by arrows were obtained from the point where the $\chi(T)$ curve deviates from the broken line. Clear anomalies in the form of a downturn on cooling are observed in the vicinity of T_N for the alloys with $x = 0$, 0.6, 6.1 and 7.0, similarly to the behaviour usually observed for Cr alloys below T_N. The downturn in $\chi(T)$ on cooling through T_N is ascribed to a decrease in the density of states at the Fermi surface when the nested parts of the electron and hole Fermi sheets are annihilated. The decrease in the density of states is accompanied by a decrease in the itinerant electron concentration responsible for magnetism.

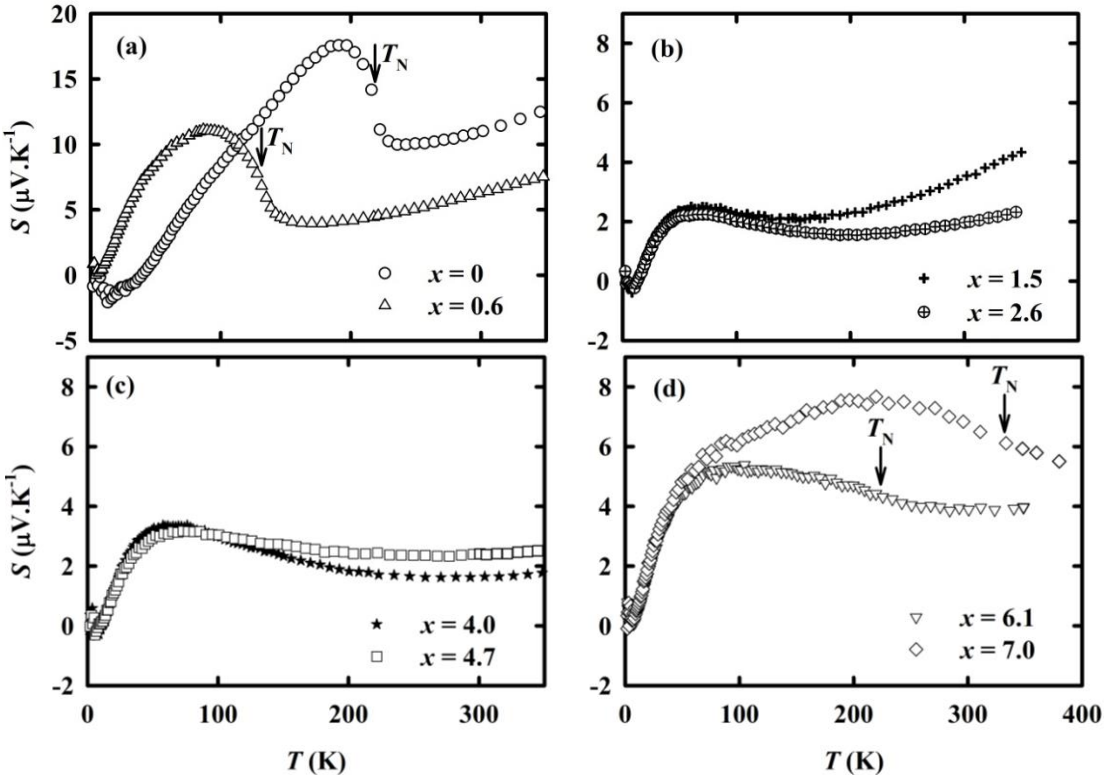

Figure 2: The temperature dependence of the Seebeck coefficient, $S(T)$, of the $(Cr_{100-x}Al_x)_{99}V_1$ alloy system with (a) $x = 0$ (○) and 0.6 (△), (b) $x = 1.5$ (+) and 2.6 (⊕), (c) $x = 4$ (★) and 4.7 (□) and (d) $x = 6.1$ (▽) and 7 (◊). The arrows indicate the positions of T_N obtained from the minimum of the (dS/dT) vs. T curves. Note the different temperature scales.

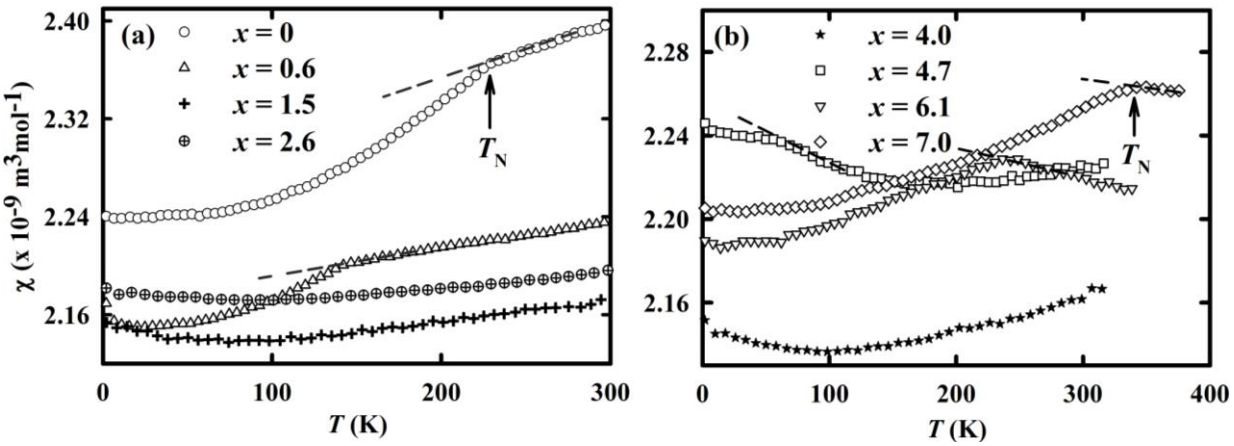

Figure 3: The temperature dependence of the magnetic susceptibility, $\chi(T)$, of the $(Cr_{100-x}Al_x)_{99}V_1$ alloy system with (a) $x = 0$ (○), 0.6 (△), $x = 1.5$ (+) and 2.6 (⊕) and, (b) $x = 4$ (★), 4.7 (□), $x = 6.1$ (▽) and 7 (◊). The experimental error in χ is approximately 0.1% emanating from measurement of the sample masses. Note the different scales in panels (a) and (b).

It is noted that the alloy with $x = 4.7$ of figure 3(b) depicts an anomaly in the form of a rather prominent upturn below a temperature of about 150 K, compared to the behaviour of alloys with $x = 1.5$, 2.6 and 4.0, despite the observation of paramagnetic behaviour in $\rho(T)$ for $x = 4$. This is taken as indication of a weak SDW AFM component for $x = 4.7$, with T_N estimated at approximately 70 K, taken at the point where the $\chi(T)$ curve deviates from the broken line. The anomalies observed in the $\chi(T)$ measurements for samples with $x > 4.7$ are better defined than those observed in the $\rho(T)$ and $S(T)$ curves. It is observed in figure 3(a) that χ increases almost linearly with temperature at $T > T_N$ for the ISDW alloys with $x < 1.5$. This is in contrast with the two $x = 6.1$ and 7.0 CSDW alloys that each depicts a downturn at $T > T_N$ and a peak in $\chi(T)$ at T_N, as is clear in figure 3(b). $\chi(T)$ peaks, followed by a broad minimum above the peak, were previously also observed by Sousa *et al*. [9] in the $Cr_{100-x}Al_x$ alloy system for CSDW alloys with $x = 2.23$ and 2.83. de Oliveira *et al*. [10] furthermore reported $\chi(T)$ peaks at T_N also in the $Cr_{100-y}V_y$ alloy system for alloys with $y \leq 0.67$. The peaks were attributed to a local SDW that is formed around the V atoms, resulting in Curie-Weiss paramagnetism above T_N [10]. This might also be the case in the present $(Cr_{100-x}Al_x)_{99}V_1$ alloy system. The minimum near 150 K in $\chi(T)$ for $x = 4.7$ of figure 3(b) is then considered as a precursor to a possible peak at T_N that is not fully realised down to 2 K in this alloy. Alloys with $x = 1.5$, 2.6 and 4.0 in figure 3 did not show anomalous behaviour associated with a magnetic transition and can be taken to be paramagnetic at all temperatures down to 2 K.

Figure 4 shows the magnetic phase diagram obtained from $\rho(T)$, $S(T)$ and $\chi(T)$ measurements on the $(Cr_{100-x}Al_x)_{99}V_1$ alloy system. It is observed that T_N decreases with an increase in Al content and is completely suppressed to below 2 K around 1.5 at.% Al. Antiferromagnetism reappears above about 4.0 at.% Al. Addition of just 1 at.% V completely suppresses antiferromagnetism in the $Cr_{100-x}Al_x$ alloy system in the concentration range $1.5 \lesssim x \lesssim 4.0$. The results indicate a phase transition from ISDW to P around 1.5 at.% Al and a P to CSDW transition around 4.0 at.% Al on increasing the Al content at 2 K.

The addition of V decreases the strength of AFM in the $Cr_{100-x}Al_x$ through a reduction of the itinerant electron concentration in the alloy system [1], while Mo suppresses AFM utilizing a different mechanism, through electron hole pair breaking effects due to electron scattering and a delocalization of the 3-d bands in Cr on introducing the 4-d bands of Mo [1]. Although the mechanisms of the suppression of AFM is different for V and Mo, it is interesting to note that the effect of 1 at.% V to the

$Cr_{100-x}Al_x$ alloy system is almost similar to that of 5 at.% Mo that suppresses AFM in the concentration range $2 \leq x \leq 5$ [5, 7]

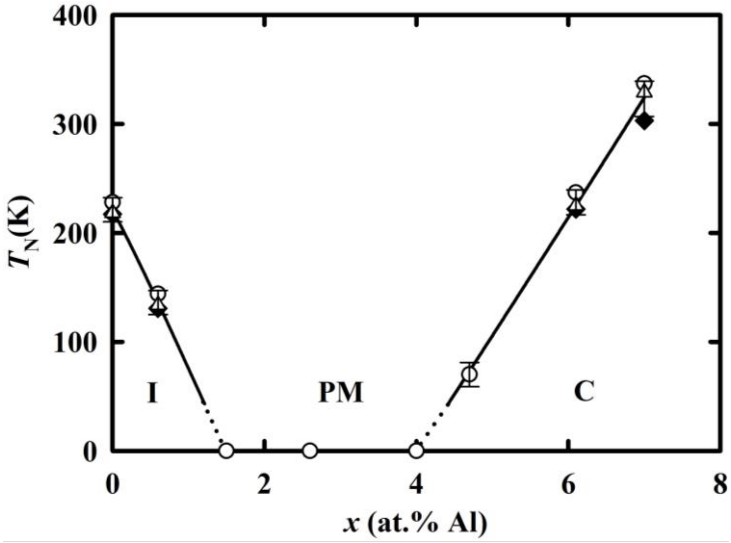

Figure 4: $(Cr_{100-x}Al_x)_{99}V_1$ alloy system in the range $0 \leq x \leq 7.0$ obtained from electrical resistivity (△), Seebeck coefficient (♦) and magnetic susceptibility (○) measurements. I, PM and C denotes incommensurate spin-density-wave, paramagnetic and commensurate spin-density-wave phases, respectively. The lines are guides to the eye through the data points. Error bars indicate the experimental errors in the determination of T_N

4. Conclusion

Electrical resistivity, Seebeck coefficient and magnetic susceptibility studies on the $(Cr_{100-x}Al_x)_{99}V_1$ showed that AFM in the alloy system is completely suppressed to below 2 K in the concentration range $1.5 \lesssim x \lesssim 4.0$. The results indicate an ISDW-P phase transition around 1.5 at.% Al and a P-CSDW phase transition around 4.0 at.% Al. The magnetic anomalies observed in the magnetic susceptibility measurements of the present study pin-point T_N in general more precisely than in the electrical resistivity and Seebeck coefficient measurements. $\chi(T)$ measurements therefore provide a useful tool in probing magnetic properties in this alloy system. Furthermore, the peak in the $\chi(T)$ measurements for alloys with $x > 4.7$ suggest the presence of a local magnetic moment component in $\chi(T)$ of the present $Cr_{100-x}Al_x)_{99}V_1$ alloy system, similar to that previously reported for $Cr_{100-x}Al$ and $Cr_{100-y}V_y$ alloys. The magnetic properties of the present alloy system mirrors that of the $(Cr_{100-x}Al_x)_{95}Mo_5$ system that suppresses AFM in the concentration range $2 \leq x \leq 5$.

References

[1] Fawcett E, Alberts H L, Galkin V Y, Noakes D R and Yakhmi J V 1994 *Rev. Mod. Phys*. **66** 25
[2] Lomer W M 1962 *Proc. Phys. Soc. (London)* **80** 489
[3] Baran A, Alberts H L, Strydom A M, and du Plessis P de V 1992 *Phys. Rev. B* **45** 10473
[4] Alberts H L, Prinsloo A R E and Strydom A M 2010 *J. of Magn. Magn. Mater*. **322 1092**
[5] Smit P and Alberts H L 1986 *J. Phys. F* **16** L191
[6] Alberts H L and Burger S J 1978 *Solid State Commun*. **28** 771.
[7] Muchono B, Prinsloo A R E, Sheppard C J, Alberts H L and Strydom A M *Proc. SAIP2011* 220
[8] Trego A L and Mackintosh A R 1968 *Phys. Rev*. **166** 495
[9] Sousa J B, Amado M M, Pinto R P, Pinheiro M F, Braga M E, Moreira J M, Hedman L E, Åström H U, Khlaif L, Walker P, Garton G and Hukin D 1980 *J .Phys. F: Metal Phys*. **10** 2535
[10] de Oliveira A J A, Ortiz W A, de Lima, O F and de Camargo P C 1997 *J. Appl. Phys*. **81** 4209